

# Spectral reproduction from scene to hardcopy I: Input and Output

Francisco Imai,<sup>a</sup> Mitchell Rosen,<sup>a</sup> Dave Wyble,<sup>a</sup> Roy Berns<sup>a</sup> and Di-Yuan Tzeng<sup>b</sup>

<sup>a</sup> Munsell Color Science Laboratory, RIT, Rochester, NY

<sup>b</sup> Applied Science Fiction, Austin, TX

## ABSTRACT

Efforts to construct end-to-end color reproduction systems based on the preservation of scene spectral data have been underway at the Munsell Color Science Laboratory (MCSL). The goal is to present hardcopy results which are spectrally matched to original colors. The evaluated approach consists of capturing scenes through a trichromatic digital camera combined with multiple filterings followed by an image processing stage and then four-color printing. The acquisition end is designed to estimate original scene spectra on a pixel-by-pixel basis based on system characterizations which takes into account the camera sensitivities as modulated by the filterings and scene colorant make-up. The spectral-based printing used in this research is able to produce the least metameric reproduction to the original scene using a computationally feasible approach. Results show a system accuracy of mean  $\Delta E^*_{94}$  of 1.5 and spectral reflectance rms error of 0.9%.

**Keywords:** multi-spectral imaging, multi-channel image acquisition, spectral printing, spectral reproduction, MVSI

## 1. LIMITATIONS OF TRADITIONAL IMAGE REPRODUCTION SYSTEMS

Current graphic arts reproduction techniques of image capture, scanning, proofing and printing are still heavily entrenched in the traditions of densitometry and crafts experience. Color Management Systems which rely on colorimetry find use. Particularly the MARC project in European museums showed the feasibility of an end-to-end scene to hardcopy colorimetric color management system for artwork reproduction.<sup>1</sup> This project was very successful in producing high-quality reproductions that matched the original painting under controlled illumination. These approaches can be used to produce pleasant hardcopy or an accurate hardcopy under a controlled environment, but for critical color-matching applications such as catalog sales and art-books these techniques can often lead to color reproductions which lack appropriate accuracy. Multi-channel Visible Spectrum Imaging (MVSI), also known as *spectral imaging*, offers better accuracy at the expense of more system complexity and higher system bandwidth demands.<sup>2-6</sup> Developing an MVSI color reproduction system is described here.

A variety of camera approaches are available for MVSI systems.<sup>7-15</sup> The Munsell Color Science Laboratory (MCSL) has given a great deal of attention to two different general categories. The first is a narrow band approach.<sup>7-11</sup> Results have been reported on the use of placing a narrow bandpass tunable filter in front of a monochrome sensor.<sup>10, 11, 15</sup> Both CCD<sup>15</sup> and panchromatic black and white film<sup>11</sup> have been utilized as such sensors. These systems are analogous to using a spectrophotometer sampling the visible spectrum at known bandpass and wavelength interval. The second category, which has received a large amount of attention from the MCSL, has been a general wide band approach.<sup>12-15</sup> Again, a number of publications have reported the results of using a conventional trichromatic digital camera combined with absorption filters or different light sources.<sup>13-15</sup> In this broad-band approach the spectral reflectance of each pixel of the original scene can be estimated using *a priori* spectral analysis with direct measurement and imaging of samples of the object to establish a relationship between the digital counts and spectral reflectance. The wide-band acquisition takes advantage of the possibility to decrease the spectral sampling increment without a significant loss of spectral information because of the absorption characteristics of both man-made and natural colorants.<sup>16-21</sup>

The image processing stage of the MVSI system involves the spectral reflectance estimation using the captured multi-channel data followed by transformation to digits appropriate for the output medium. In many cases where the mathematics needed to estimate reflectance from captured digits is purely linear,<sup>22</sup> the processing to estimate the spectral reflectance is computationally fast even for high-resolution images. When the output processing goal is to minimize metamerism between the original and the rendered image, the subsequent image processing can be extremely complex. A companion paper to this one<sup>23</sup> describes one approach which makes such complex processing feasible.

In contrast to the abundance of research concerning image capture aspects of spectral imaging, there are few works reported on the spectral color reproduction of hardcopy.<sup>11, 24, 25</sup> At MCSL, an algorithm was developed by Tzeng comprising many steps.<sup>24</sup> At first, *a priori* analysis is performed to determine an optimal ink set.<sup>26</sup> In this analysis, the spectral properties of the colorants used to create the original object are measured or estimated and analyzed statistically. The possible statistical colorants are correlated to real inks in an existing database resulting in an optimal ink set.<sup>27</sup> A printer overprint model is next derived<sup>28</sup> The spectral reflectance of the ink overprints are predicted using Kubelka-Munk theory.<sup>29</sup> The Yule-Nielsen

modified Neugebauer equations are used to predict spectral reflectance from dot areas. More details on the use of this model for developing printer profiles are given by Iino and Berns.<sup>30,31</sup> Using this approach Tzeng was successful in reproducing the colors of the GretagMacbeth ColorChecker rendition chart using the Dupont WaterProof printing process with six inks.<sup>24</sup> The average  $\Delta E^*_{94}$  color difference between the original rendition chart and the reproduction for illuminant D50 and the 2 degree observer was 1.9 and the maximum value was 5.8. The research by Tzeng was fundamental and not focused on the high-speed requirements to create color separations for high-resolution images. Essentially, Tzeng used images with hundreds of pixels (corresponding to the various target colors such as the ColorChecker). Extending his research to images with millions of pixels is a currently underway.<sup>23,32</sup> To improve our research efficiency, we have replaced the six-color WaterProof system with a four-color ink-jet printer. In the future, this will be replaced with a six-color ink-jet printer. The remainder of this publication will be limited to four-color hardcopy.

We have developed an end-to-end spectral reproduction from scene to hardcopy comprising a spectral image acquisition system and a spectral-based printing system. Our MVSI color reproduction system is shown in Figure 1. A scene is captured using a multi-channel imaging of the visible spectra. The spectral reflectance of each pixel is estimated from the digital counts. The spectral reflectance image is processed by the spectral-based color separation minimizing metamerism in order to yield color separations that are finally printed. The printed reproduction, in theory, will spectrally match the original scene objects (assuming sufficient degrees of freedom in ink selection). The remainder of this publication will focus on the wide band approach using trichromatic digital camera and multi-filtering for the multi-channel imaging of the visible spectra. In this case, the spectra reflectance estimation was performed using the multi-channel data and *a priori* information derived by eigenvector analysis of the imaged target.

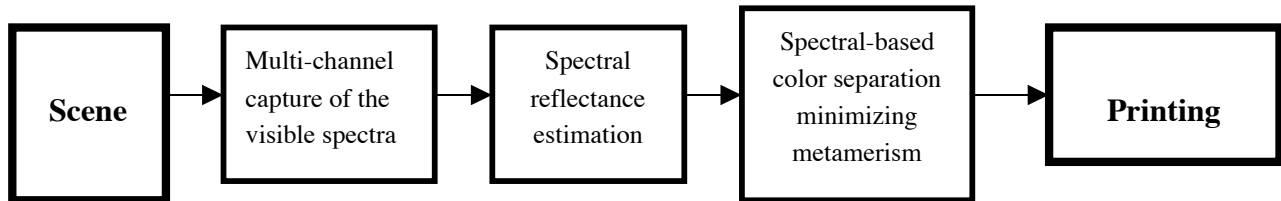


Figure 1. MVSI color reproduction block diagram

## 2. EXPERIMENTAL

In our experiments, we used a medium-spatial resolution trichromatic IBM PRO\3000 digital camera system (3,072 x 4,096 pixels, R, G, B filter wheel, dark current corrected 12 bits per channel that has a 45°/0° imaging configuration using tungsten illumination).<sup>33</sup> The spectral sensitivities of the IBM PRO\3000 digital camera system were measured, as well as the spectral radiant power of the camera-taking illuminant. White spatial correction is performed to the captured image to account for spatial non-uniformity of the illumination. For the printer we used an Epson Photo Style 1200 ink-jet printer; although it has six ink capability, only the CMYK inks were used. Given that a target such as the GretagMacbeth ColorChecker rendition chart has many out-of-gamut colors,<sup>24</sup> a target was created using the ink-jet printer, thus insuring all colors were in gamut. A target with 55 patches using color along some hue axes was generated. The color distribution of our target in CIELAB space for D50 illuminant and 2 degrees observer is shown in Figure 2. All the spectral measurements were performed using a Gretag Spectrolino 45°/0° spectrophotometer that reports accuracy of 0.12  $\Delta E^*_{94}$  units (D50 illuminant and 2° observer). Five hardcopies of the target were printed using the Epson printer. The printer repeatability was tested calculating the color difference of the measured spectral reflectance between the prints. The average  $\Delta E^*_{94}$  calculated for D50 and the 2° observer was 0.23 and the maximum value between any corresponding measurement was 1.1  $\Delta E^*_{94}$  units. Considering that this result includes measurement error, we conclude that the printer can repeat the same colors with sufficient accuracy.

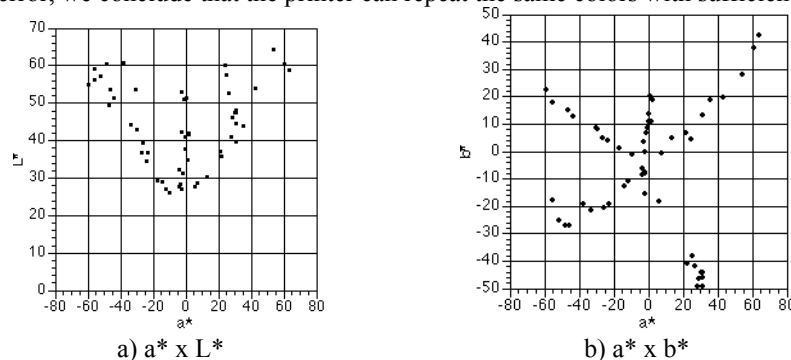


Figure 2. Colorimetric plots for the target with 55 patches (D50 illuminant, 2° observer).

The evaluation of the color accuracy of our MVSJ color reproduction system was divided in three parts: evaluation of the spectral reflectance estimation of the MVSJ acquisition system, the evaluation of the MVSJ spectral-based printing minimizing metamerism, and the evaluation of the MVSJ color reproduction system comprising both acquisition and printing stages.

The accuracy of the spectral estimation from the multi-channel acquisition can be evaluated starting from the analysis of the eigenvector reconstruction and concluding with estimation from the camera. The evaluation of the spectral reflectance of the MVSJ acquisition system is then subdivided in three parts as shown in Figures 3, 4 and 5. Figure 3 shows the theoretical evaluation of eigenvector analysis. Eigenvector analysis is evaluated theoretically reconstructing the spectral reflectances from the derived eigenvectors and eigenvalues and comparing the estimated reflectances with the measured spectral reflectances.

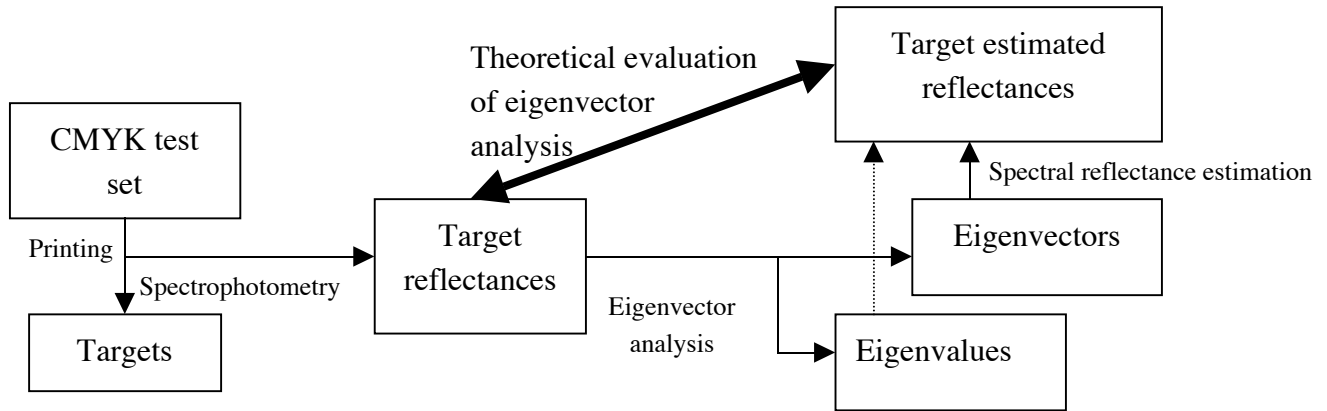


Figure 3. Block diagram of the theoretical evaluation of the eigenvector analysis performance.

Figure 4 shows the evaluation of the spectral estimation from the simulated digital counts.

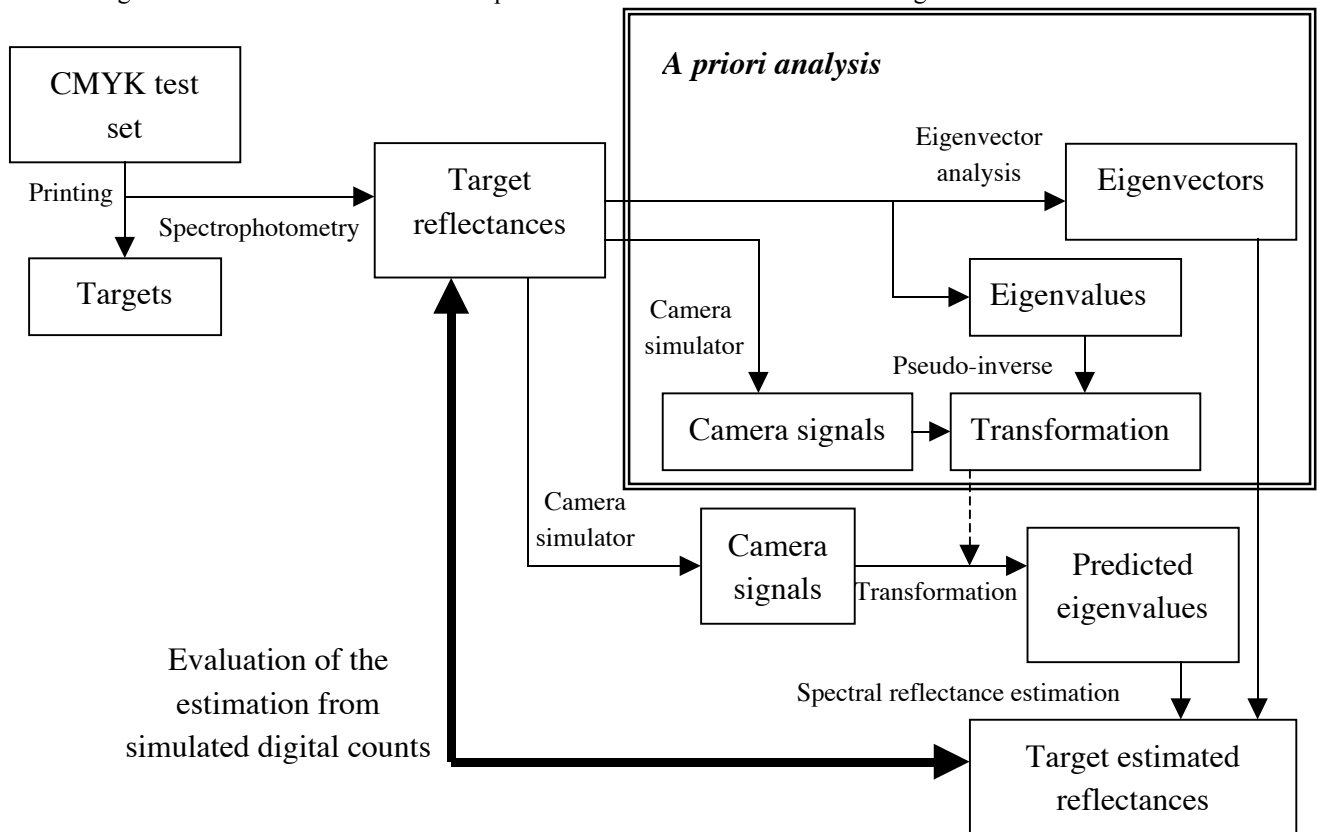
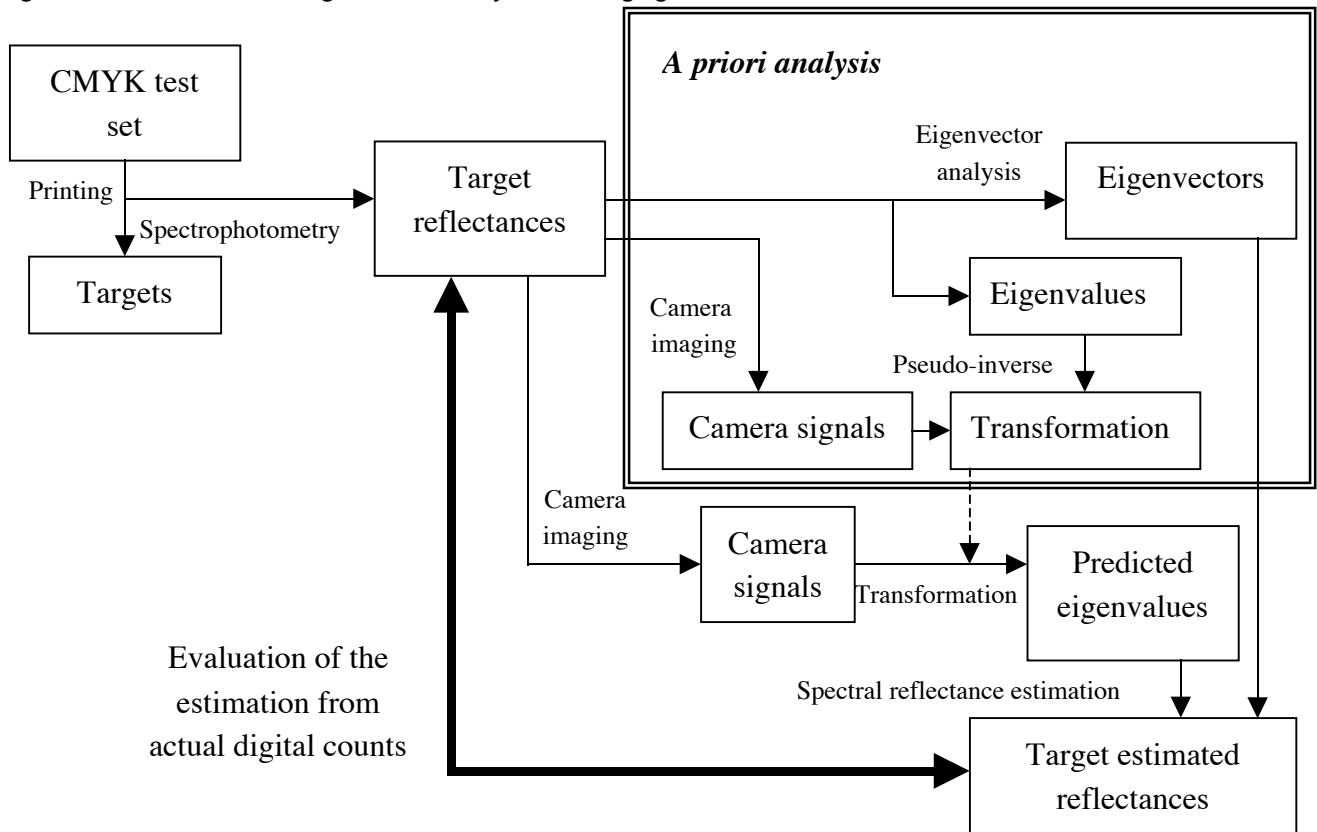


Figure 4. Block diagram of the spectral estimation from simulated digital counts.

After doing eigenvector analysis, it is possible to simulate the digital counts using a camera model given by  $C=(DF)^T Sr$ , where  $D$  is the camera spectral sensitivities,  $F$  is the spectral transmittance of the filters,  $S$  is the illumination spectral power distribution,  $r$  is the object spectral reflectance, and  $C$  is the simulated digital counts. The transformation derived by *a priori* analysis is used to reconstruct the spectral reflectances from the simulated digital signals and eigenvectors. The spectral estimation is evaluated comparing the estimated spectral reflectances and the measured spectral reflectances. The estimation of the spectral reflectance using simulated digital counts gives a performance of the spectral estimation without introducing noise from the imaging

Figure 5 shows the evaluation of the spectral estimation from the actually measured digital counts from the averaged patches of the captured image. As in the evaluation of the spectral estimation using simulated camera signals, the estimation of the spectral reflectance using actual digital signals also relies on *a priori* spectral analysis but instead of using simulated digital counts it uses camera signals obtained by actual imaging.



**Figure 5.** Block diagram of the spectral estimation from actually measured digital counts from averaged patches captured by the camera.

The evaluation of the spectral-based printing system minimizing metamerism can be subdivided in two different evaluation experiments. In the first experiment, shown in Figure 6, we evaluate the accuracy of the optimization calculation to estimate the color separations from the spectral reflectances in our printing model. In order to avoid any noise introduced by printing and subsequent measurement of spectral reflectances the spectral reflectances were simulated. At first, the input spectral reflectances of the target are simulated using the printer forward model and they are used in the printer inverse model to predict the CMYK color separations. The output spectral reflectances are simulated from the color separations using the printer forward model. Then the input and output simulated spectral reflectances are used to evaluate the model used in the spectral-based printing.

In the second experiment, shown in Figure 7, we evaluate the accuracy of the spectral-based printing system minimizing metamerism. At first, a target is printed in the printer. The spectral reflectances of the targets are measured and they are used in the printer inverse model to predict the CMYK color separations. Then, the target is reproduced by directly sending the CMYK dot areas to the printer. The spectral reflectances of the printed targets are measured. The measured spectral reflectances of the originally printed target and the reproduced target are compared.

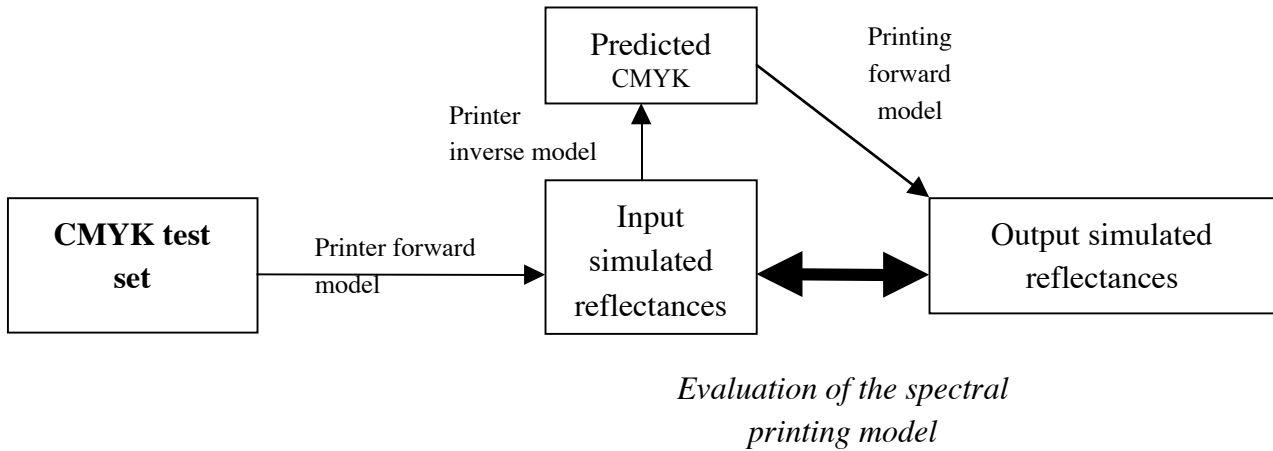


**Figure 6.** Block diagram of the evaluation of the model used in the spectral-based printing.

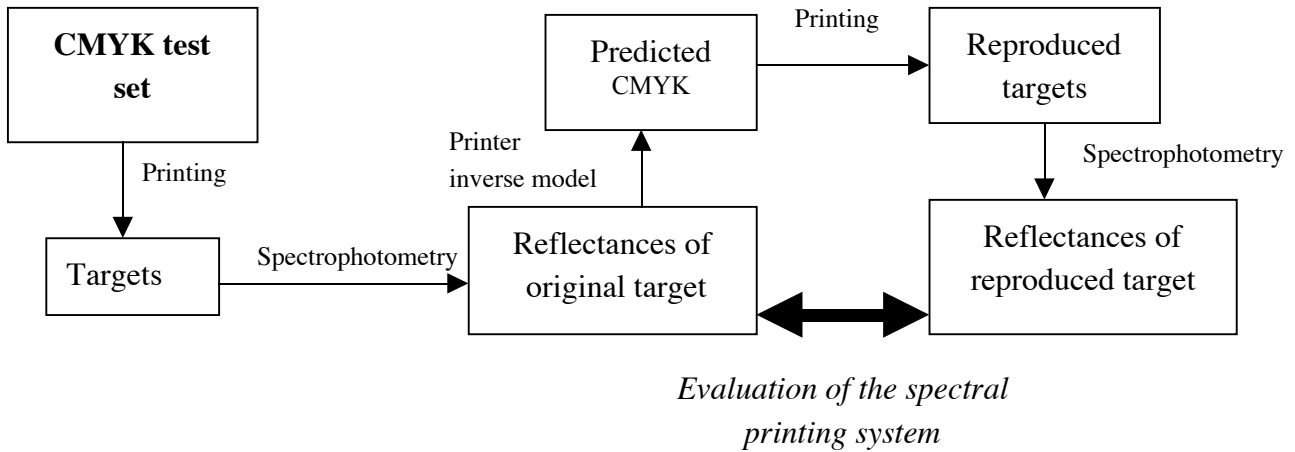


**Figure 7.** Block diagram of the method of evaluation for the spectral printing system.

Finally the end-to-end spectral reproduction system is evaluated using the method shown in Figure 8. At first, a target is printed in the designated printer. The printed target is imaged by a digital camera and the spectral reflectance estimated from the digital counts. Then, the estimated spectral reflectances are processed by the printer inverse model in order to give the color separations that are printed to get the reproduction of the targets whose spectral reflectances are measured for the comparison with the originally printed targets.

### 3. RESULTS

The spectral reflectances of the printed targets with 55 patches were measured and eigenvector analysis was performed. Table I shows the cumulative contribution for each multiple-of-three eigenvectors and the influence of the number of eigenvectors on the colorimetric accuracy and spectral accuracy of the spectral reconstruction. The colorimetric accuracy is calculated using CIE94 for D50 and the 2° observer.

From Table I it is possible to notice that 6 eigenvectors can reconstruct the original spectral with 99.97% of accuracy. From colorimetric and spectral evaluation we can conclude that the use of six eigenvectors to reconstruct spectra is a compromise between accuracy and our aim of reducing the number of channels. Theoretically, using six eigenvectors to reconstruct spectra gives colorimetric error less than one  $\Delta E^*_{94}$  unit and spectral reflectance rms error less than 1%. Figure 9 shows the histogram of  $\Delta E^*_{94}$  for D50 and the 2° observer between the measured and predicted spectral reflectances when 6 eigenvectors are used in the spectral estimation. These results correspond to the analysis shown in Figure 3.

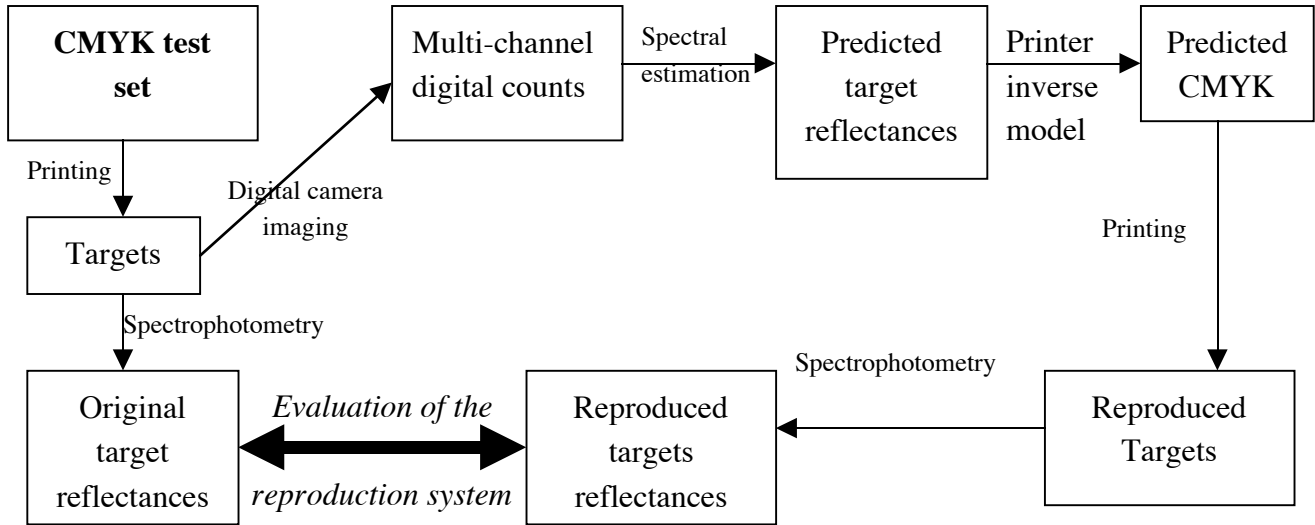


**Figure 8.** Block diagram of the method of evaluation for the end-to-end spectral reproduction system from original to hardcopy.

**Table I.** Cumulative variance contribution and influence of the number of eigenvectors used in the spectral reconstruction of printed targets on the colorimetric and spectral error.  $\Delta E^*_{94}$  calculated for D50 and the 2° observer of the eigenvectors in reflectance space. It corresponds to the block diagram of Figure 3.

Number of eigenvectors	Cumulative variance contribution (%)	Mean $\Delta E^*_{94}$ (D50, 2°)	Spectral reflectance rms error factor
3	98.10	4.3	0.027
6	99.97	0.4	0.008
9	99.99	0.1	0.004
12	100.00	0.1	0.002

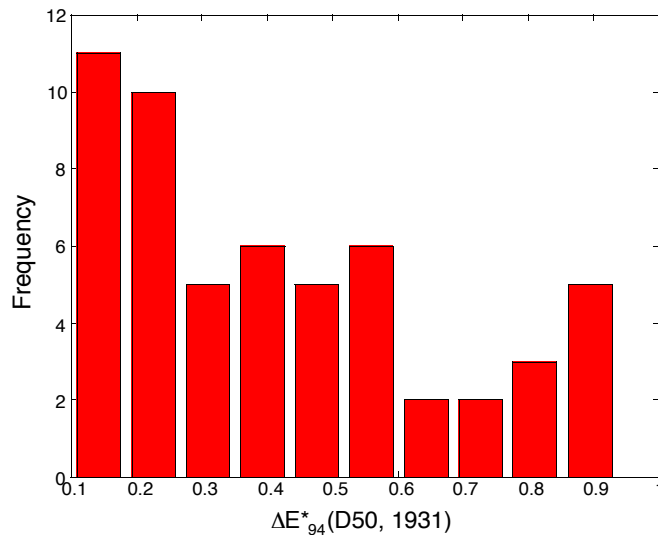


**Figure 9.** Histogram of  $\Delta E^*_{94}$  for D50 and the 2° observer between the measured and predicted spectral reflectances when 6 eigenvectors are used in the spectral estimation. It corresponds to the method in the block diagram of Figure 3.

### 3.1 Estimation of spectral reflectance using simulated and measured digital counts

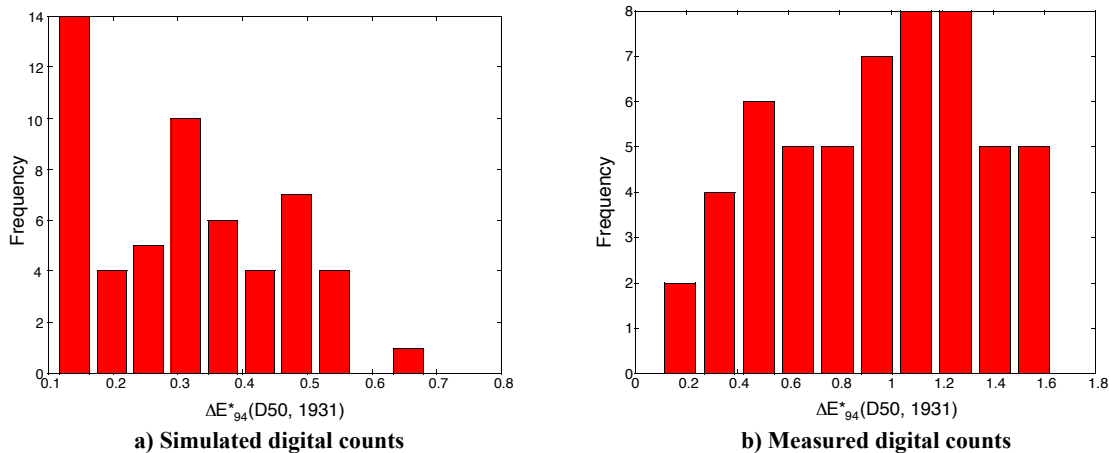
The measured spectral properties of the IBM PRO\3000 digital camera system were used to simulate the digital counts using the spectral transmittance of the Kodak Wratten filter number 38 (Light Blue). The performance for the trichromatic system without filtering and with the light-blue filter give 6 signals that were used with 6 eigenvectors of the spectral reflectance of each target in order to estimate the spectral reflectances from digital counts. Table II shows the colorimetric and spectral accuracy for the printed ink targets.  $\Delta E^*_{94}$  calculation was performed for illuminant D50 and 2° observer. The metameric index was calculated using the Fairman metameric black method, between standard illuminants D50 and A using  $\Delta E^*_{94}$  in the calculations.<sup>34</sup>

Table II shows the colorimetric and spectral performances of the spectral estimation for the printed ink targets using 6 eigenvectors of each target and measured digital counts from 2 sets of trichromatic signals (R, G, B without filter and R, G, B with light-blue Wratten absorption filter number 38), using IBM PRO\3000 digital camera system.

**Table II.** Spectral reconstruction of the printed ink target using 6 eigenvectors and 6 digital counts from IBM PRO\3000 digital camera system. The simulated digital counts were obtained combined the trichromatic camera without filter and with light blue filter and corresponds to the method described in Figure 4. The measured digital counts were obtained combining the trichromatic camera without a filter and with the light-blue filter and corresponds to the method described in Figure 5.

Results	Estimation from simulated digital counts			Estimation from measured digital counts		
	$\Delta E^*_{94}$ (D50, 2°)	reflectance factor rms error	Metameric Index ( $\Delta E^*_{94}$ ) (D50, A)	$\Delta E^*_{94}$ (D50, 2°)	reflectance factor rms error	Metameric Index ( $\Delta E^*_{94}$ ) (D50, A)
<b>Average</b>	<b>0.3</b>	<b>0.010</b>	<b>0.1</b>	<b>0.9</b>	<b>0.014</b>	<b>0.4</b>
<b>Standard deviation</b>	0.1	0.003	0.08	0.4	0.004	0.2
<b>Maximum</b>	0.7	0.020	0.3	1.6	0.026	1.0
<b>Minimum</b>	0.1	0.006	0.02	0.1	0.007	0.005

It is possible to see from Table II that the estimation of spectral reflectance from 6 simulated digital counts and 6 eigenvectors produced very accurate colorimetric and spectral predictions. Comparing Tables I and II it is possible to see that the spectral estimation using simulated digital counts performed worse than the pure theoretical calculations using eigenvectors. This was expected because the introduction of the digital camera system adds error caused by quantization and slight lack of fit between scalars and digital counts. Moreover, Table II shows that the performance was worse in the reconstruction using measured digital counts than the reconstruction using simulated digital counts. This result was also expected because of the introduction of noise and typical experimental uncertainty. Figure 10 shows the histogram of  $\Delta E^*_{94}$  for D50 and the 2° observer between the measured and predicted spectral reflectances for both methods using simulated and measured digital counts.



**Figure 10.** Histogram of  $\Delta E^*_{94}$  for D50 and the 2° observer between the measured and predicted spectral reflectances when 6 eigenvectors and digital counts from IBM PRO/3000 are used in the spectral estimation. The histograms a) and b) were obtained using the methods described respectively in Figures 4 and 5.

Figure 11 shows a comparison of the spectral curves of one of the reproduced patches of the printed ink target. The measurement of the original reflectance is compared with the reflectance estimated only by eigenvectors, the reflectance estimated by simulated digital counts, and the reflectance estimated by measured digital counts. From Figure 11 it is possible to see that the reflectance estimated using eigenvectors was almost a perfect match with the measured reflectance. Adding progressively more uncertainty to the estimation first using simulated digital counts and then measured digital counts in the estimation produced spectral curves that diverged progressively from the measured reflectance, as expected.

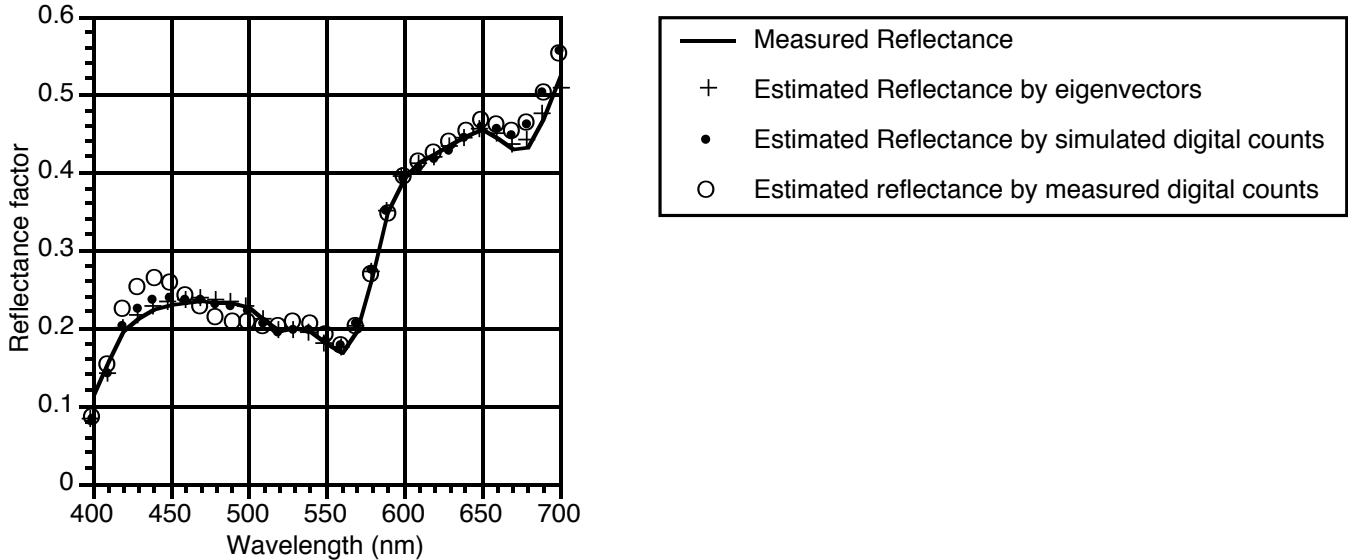


Figure 11. Comparison of spectral reflectance curves between the original (measured) and the estimation using only eigenvectors, estimation by simulated digital counts and estimation by measured digital counts.

### 3.2 Evaluation of the spectral-based printing model and printing system

The method for evaluating the optimization used in our model described in Figure 6 was implemented using the Matlab 5.3 fmincon optimization tool. The rms error factor between the simulated input spectral reflectance and the simulated output spectral reflectance was used as the cost function. The maximum number of iterations was chosen to be 50. In terms of speed performance, it was possible to process, on average, 7 pixels per second using 8 processors of a SGI Onyx 2. Table III shows the colorimetric and spectral accuracy of the optimization for our printed ink target with 55 patches. There was a problem of convergence in the optimization for one patch and it was excluded from the analysis of the results.

We used the same software and parameters set to evaluate the model (optimization) performance to the spectral-based printing system described in Figure 7. Table III also shows the colorimetric and spectral accuracy of the spectral-based printing system for the target with 55 patches. In this case we also excluded one patch due to a convergence problem. Figure 12 shows the histogram of  $\Delta E^*_{94}$  for D50 and the  $2^\circ$  observer between the original and predicted spectral reflectances for the printer model evaluation and the spectral printing system.

Table III. Evaluation of the spectral-based printing model and the printing system. The evaluation of the optimization used in the printing model corresponds to the method described in Figure 6. The evaluation of the spectral-based printing corresponds to the method described in Figure 7.

Results	Evaluation of the optimization (model)			Evaluation of the spectral-based printing		
	$\Delta E^*_{94}$ (D50, $2^\circ$ )	reflectance factor rms error	Metameric Index ( $\Delta E^*_{94}$ ) (D50, A)	$\Delta E^*_{94}$ (D50, $2^\circ$ )	reflectance factor rms error	Metameric Index ( $\Delta E^*_{94}$ ) (D50, A)
Average	0.4	0.001	0.04	1.0	0.007	0.1
Standard deviation	0.8	0.002	0.05	1.0	0.005	0.1
Maximum	3.5	0.010	0.22	4.1	0.020	1.4
Minimum	0.0	0.0003	0.00	0.1	0.002	0.0

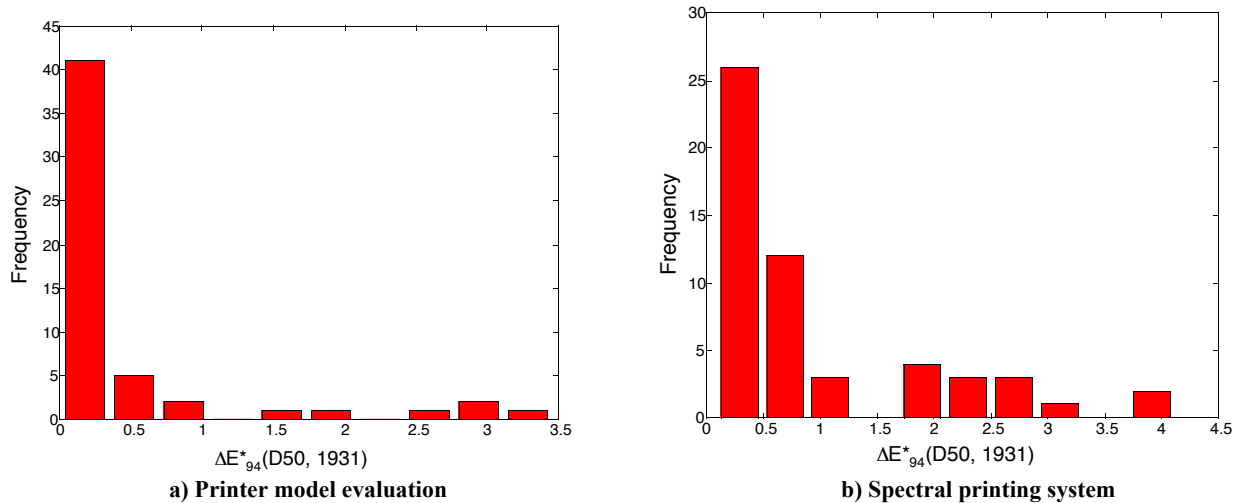


**Figure 12.** Histogram of  $\Delta E^*_{94}$  for D50 and the 2° observer between the original and predicted spectral reflectances for the printer model evaluation and the spectral printing system, respectively corresponding to the evaluation in Figures 6 and 7.

From Table III and Figure 12 it is possible to conclude that the printer model is working with a reasonable accuracy in terms of colorimetric and spectral error. The evaluation of the spectral printing system presented slightly worse results as expected because it includes actual printing and spectral reflectance measurements.

Figure 13 shows a comparison of spectral reflectance curves between the measured spectral reflectance before the spectral printing model, the spectral reflectance simulated from the color separations (input), the spectral reflectance simulated from the predicted color separations (output), and the spectral reflectance measured from the printed targets after the spectral printing model. From the figure it is possible to see that the simulated spectral reflectance before and after the printing model matches well showing that the printer model works accurately. The spectral curves diverge progressively from the measured spectral reflectance (before spectral printing) as we add at first the printing model and to the measured spectral reflectance (after spectral printing) that includes printing and measurement uncertainty.

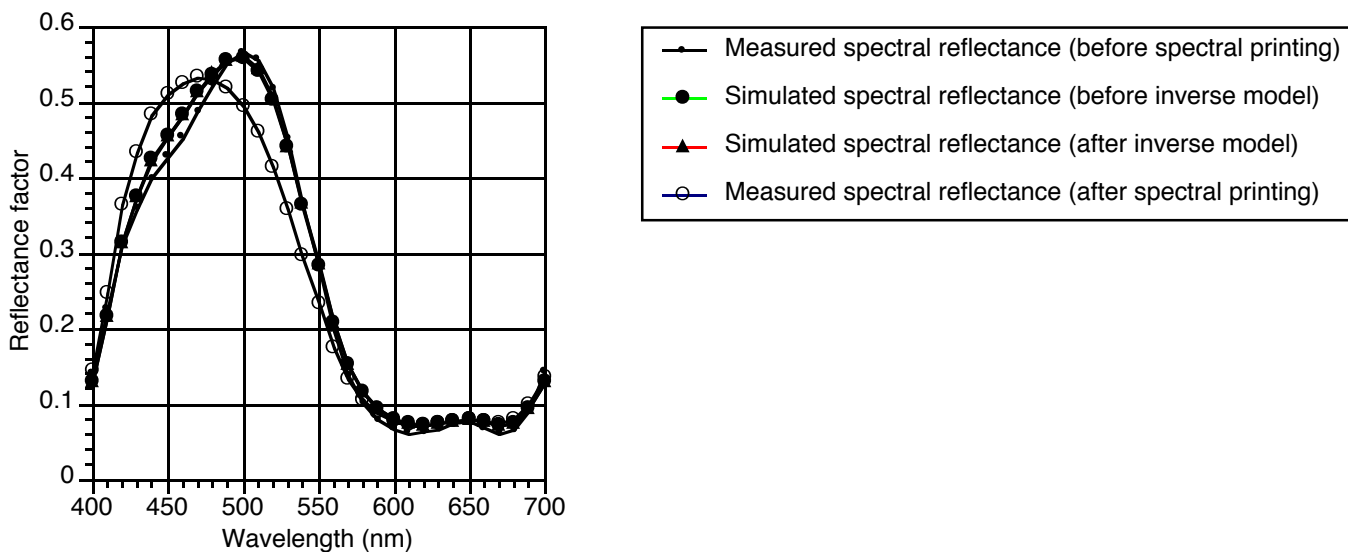


**Figure 13.** Comparison of spectral reflectance curves between the measured spectral reflectance before the spectral printing model, the spectral reflectance simulated from the color separations (input), the spectral reflectance simulated from the predicted color separations (output) and the spectral reflectance measured from the printed targets after the spectral printing model.

### 3.3 Spectral-based reproduction system from original to hardcopy

Finally we evaluated the performance of the whole spectral-based system from the originally printed ink targets through the multi-channel spectral imaging, spectral reflectance estimation, spectral-based color separation and printing. Table IV

summarizes the colorimetric and spectral accuracy of the spectral-based printing system for the target with 55 patches. It corresponds to the method represented in Figure 8.

**Table IV** . Spectral reconstruction of the targets with 55 patches using a Epson Photo Stylus 1200 printer with four colors (CMYK). The spectral reflectance of the patches were estimated using six channels of IBM PRO/3000 digital camera signals (obtained combined the trichromatic signal without filtering and with light-blue Kodak Wratten absorption filter). Six eigenvectors from the target were used in the spectral estimation. It corresponds to the diagram of Figure 8.

Results	$\Delta E^*_{94}$ (D50, 2°)	reflectance factor rms error	Metameric Index ( $\Delta E^*_{94}$ ) (D50, A)
Average	1.5	0.009	0.2
Standard deviation	1.2	0.005	0.1
Maximum	6.1	0.028	0.6
Minimum	0.3	0.003	0.01

Figure 14 shows the histogram of  $\Delta E^*_{94}$  for D50 and the 2° observer between the originally measured spectral reflectances and the measured reflectances of the reproduced target. Figure 15 shows two examples (best and worst match) of spectral match between original target and reproduced target. From the results in Table IV and Figure 14 and 15 we can conclude that our MVSI to match the spectral reflectance of the original scene to a hardcopy worked well demonstrating the feasibility of the spectral reproduction system.

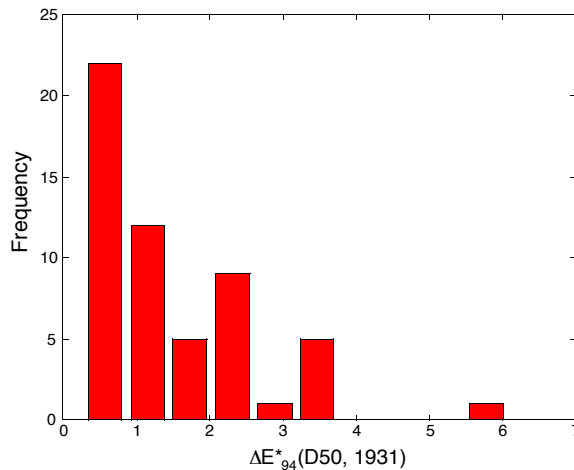


**Figure 14.** Histogram of  $\Delta E^*_{94}$  for D50 and the 2° observer between the originally measured spectral reflectances and the measured reflectances of the reproduced target. It corresponds to the diagram of Figure 8.

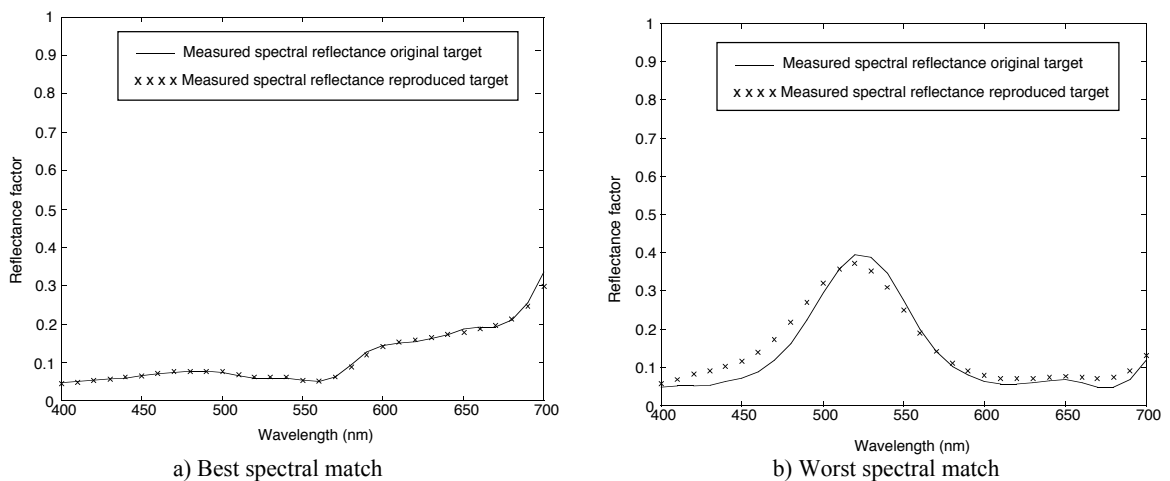


**Figure 15.** Examples of spectral matches between original target and reproduced target using the spectral reproduction system.

#### 4. DISCUSSION

Conventional four-color printing systems are limited in terms of degrees of freedom in representing the properties of spectral information. Therefore there are limitations in trying to minimize metamerism using four-color printing. The existing multiple-ink hardcopy systems that uses more than four inks (whose primary focus is expanding the color gamut) do not address the problem of metamerism since their color separation algorithms are trichromatic and not spectral in nature. If the printer has a large set of inks from which to choose from, it should be possible to select a subset of inks that achieve a spectral match between original objects and their printed reproductions by spectral reflectance image estimation, ink selection minimizing metamerism, and spectral-based printing models including separation algorithms. We believe it is possible to get more accurate results using 6 ink printing systems rather than our present 4 ink printing system.

The spectral matching capabilities of the spectral-based printing system would require far more computational power than that needed for the traditional metameric approach. Our companion paper<sup>23</sup> discusses efficient approaches to process images where tradeoffs can be biased among desired precision, processing time requirements, and available computational power and memory constraints. It could be achieved by reducing the dimensionality demands of spectral color management,<sup>32</sup> building low-dimensional lookup tables. Without such approaches, spectral color management would remain a very slow process or would make memory demands far exceeding current capabilities. A prototype system was already implemented using some of these techniques using a proofing system to produce multi-ink prints.<sup>11</sup> We are currently implementing the spectral-based color printing system using a six-color ink-jet printer that process images more efficiently.

#### 5. CONCLUSIONS

The research presented in this paper is part of our effort to integrate multi-spectral imaging capture with multi-ink printing. In the image acquisition side, the performance of the wide band acquisition system was verified by imaging a printed ink target. The performance was evaluated in terms of colorimetric accuracy (mean  $\Delta E^*_{94}$ ), spectral reflectance factor rms error and metamerism index. The experiments were performed in three steps: spectral analysis, spectral reconstruction using simulated camera signals and spectral reconstruction using measured digital counts. The spectral analysis shows the theoretical feasibility of using eigenvector analysis to reconstruct reflectance spectra. The spectral reconstruction using simulated camera signals allows the analyses of the results without signal noise introduced by the camera during imaging. Our spectral estimation based on the averaged digital counts presented a colorimetric accuracy of mean  $\Delta E^*_{94}$  of 0.9 and spectral reflectance rms error of 1.4% when the measured spectral reflectances of the printed targets were compared to the estimated spectral reflectances using the digital counts provided by our camera system and information provided by *a priori* eigenvector analysis of the target. The printing system was evaluated also progressively, first estimating the accuracy of the spectral printing model using only simulated spectral reflectances generated by the printer forward model and then evaluating the spectral printing algorithm accuracy comparing measured original and reproduced reflectances. The spectral-based printing presented remarkably good performance. Our spectral-printing system presented a colorimetric accuracy of mean  $\Delta E^*_{94}$  of 1.0 and spectral reflectance rms error of 0.7% when the measured spectral reflectances were compared to the measured spectral reflectance of the hardcopy. Finally, the entire spectral reproduction system from end-to-end presented a colorimetric accuracy of mean  $\Delta E^*_{94}$  of 1.5 and spectral reflectance rms error of 0.9%. It shows the feasibility of our spectral reproduction system.

#### 6. ACKNOWLEDGEMENTS

The authors would like to express their gratitude to DuPont for their support of this research. We would also like to acknowledge the work of many members of the Munsell Color Science Laboratory who are working on building our end-to-end spectral-based system.

#### 7. REFERENCES

1. J. Cupitt, K. Martinez, and D. Saunders, "A methodology for art reproduction in colour: the Marc project", *Computers and the History of Art* **6**, pp. 1-19, 1996.
2. B. Hill, "Aspects of total multispectral image reproduction systems", *Second International Symposium on Multispectral Imaging and High Accurate Color Reproduction*, Chiba University, pp. 67-78, 2000.
3. Y. Miyake, Y. Yokoyama, "Development of Multispectral and Color Imaging System for Recording of Art Painting", *Proc. of SPIE 3648*, pp. 190-192 and 218-225, 1999.
4. R. S. Berns, F. H. Imai, P. D. Burns and D. Tzeng, "Multispectral-based color reproduction research at the Munsell Color Science Laboratory", *Proc. SPIE Europto Series 3409*, Zürich, pp. 14-25, 1998.
5. F. Schmitt, H. Brettel, J. Y. Hardeberg, "Multispectral Imaging Development at ENST", *Proc. of First International Symposium on Multispectral Imaging and High Accurate Color Reproduction*, Chiba University, pp. 58-64, 1999.

6. P. Hung, "Color Reproduction Using Spectral Characterization", *International Symposium on Multispectral Imaging and Color Reproduction for Digital Archives*, Chiba University, pp. 98-105, 1999.
7. P. D. Burns and R. S. Berns, "Analysis of multispectral image capture", *Proc. of 4th IS&T/SID Color Imaging Conference*, IS&T, Springfield, VA, pp. 19-22, 1996.
8. P. D. Burns, "Analysis of image noise in multispectral color acquisition", Ph.D. Dissertation, R.I.T., Rochester, NY, 1997.
9. König, F. and Præfke, W., "The practice of multispectral image acquisition", *Proc. of SPIE 3409*, pp. 34-41, 1998.
10. S. Tominaga, "Spectral Imaging by a Multi-Channel Camera", *Proc. of SPIE 3648*, pp. 38-47, 1999.
11. M. Rosen and X. Jiang, "Lippmann2000: A spectral image database under construction", *Proc. of the International Symposium on Multispectral Imaging and Color Reproduction for Digital Archives*, pp. 117-122, 1999.
12. S. Toyooka, K. Miyazawa and M. Hauta-Kasari, "Low-dimensional multispectral image analyzing system with optimized broad-band filters", *Proc. of Second International Symposium on Multispectral Imaging and High Accurate Color Reproduction*, pp 59-66, 2000.
13. F. H. Imai and R. S. Berns, "Spectral Estimation Using Trichromatic Digital Cameras", *Proc. of International Symposium on Multispectral Imaging and Color Reproduction for Digital Archives*, Chiba University, pp. 42-49, 1999.
14. F. H. Imai, R. S. Berns and D. Tzeng, "A comparative analysis of spectral reflectance estimated in various spaces using a trichromatic camera system", *J. Imaging Sci. Tech.* **44**, pp. 280-287, 2000.
15. F. H. Imai, M. R. Rosen and R. S. Berns, "Comparison of spectrally narrow-band capture versus wide-band with a priori sample analysis for spectral reflectance estimation", *Proc. of in IS&T/SID Eight Color Imaging Conference*, IS&T, Springfield, VA, pp. 234-241, 2000.
16. L. T. Maloney, "Evaluation of linear models of surface spectral reflectance with small numbers of parameters", *J. Opt. Soc. Am. A* **10**, pp. 1673-1683, 1986.
17. T. Jaaskelainen, J. Parkkinen and S. Toyooka, "Vector-subspace model for color representation", *J. Opt. Soc. A* **7**, pp. 725-730, 1990.
18. M. J. Vrhel and H. J. Trussel, "Color correction using principal components", *Color Res. and Appl.* **17**, pp. 328-338, 1992.
19. D. S. Vent, "Multichannel Analysis Of Object-Color Spectra", M. S. Thesis, R.I.T., Rochester, NY, 1994.
20. M. J. Vrhel, R. Gershon and L. S. Iwan, "Measurement and analysis of object reflectance spectra", *Color Res. and Appl.*, **19**, pp. 4-9, 1994.
21. H. Haneishi, T. Hasegawa, N. Tsumura and Y. Miyake, "Design of color filters for recording artworks," *Proc. of IS&T's 50th Annual Conference*, IS&T, Springfield, VA, pp. 369-372, 1997.
22. D. H. Marimont, B. A. Wandell, "Linear models of surface and illuminant spectra", *J. Opt. Soc. Am. A* **9**, pp. 1905-1913 1990.
23. M. Rosen, F.H. Imai, X. Jiang and N. Ohta, "Spectral Reproduction from Scene to Hardcopy II: Image Processing", Submitted to *Electronic Imaging* 2001.
24. D. Tzeng, "Spectral-Based Color Separation Algorithm Development for Multiple-Ink Color Reproduction", Ph.D. dissertation, R.I.T., Rochester, N.Y, 1999.
25. M. Kouzaki, T. Itoh, T. Kawaguchi, N. Tsumura, H. Haneishi and Y. Miyake, "Spectral Color Reproduction for Hardcopy System by using Vector Error Diffusion Method", *Proc. of First International Symposium on Multispectral Imaging and High Accurate Color Reproduction*, Chiba University, pp. 106-109, 1999.
26. D. Tzeng, R. S. Berns, "Spectral-based ink selection for multiple-ink printing I. Colorant Estimation of Original Objects", *Proc. of Sixth IS&T/SID Color Imaging Conference*, IS&T, Springfield, VA, pp.106-111, 1998.
27. D. Tzeng, R. S. Berns, "Spectral-based ink selection for multiple-ink printing II. Optimal Ink Selection", *Proc. of Seventh IS&T/SID Color Imaging Conference*, IS&T, Springfield, VA, pp. 182-187, 1999.
28. D. Tzeng, R. S. Berns, "Spectral reflectance prediction of ink overprints by Kubelka-Munk turbid media theory", *Proc. of TAGA/ISCC Symposium in Vancouver B.C.*, pp. 682-697, 1999.
29. D. Tzeng, R. S. Berns, "Spectral-based Six-color Separation minimizing Metamerism", *Proc. of Eighth IS&T/SID Color Imaging Conference*, Springfield, VA, pp. 342-347, 2000.
30. K Iino and R. Berns, "Building Color Management Modules Using Linear Optimization I. Desktop color system *J. Imaging Sci. Tech.* **42**, pp 79-94, 1998.
31. K Iino and R. Berns, "Building Color Management Modules Using Linear Optimization II. Prepress System for Offset Printing", *J. Imaging Sci. Tech* **42**, pp. 99-144, 1998.
32. M. Rosen, M. Fairchild, G. Johnson, D. Wyble, "Color Management within a Spectral Image Visualization Tool", *Proc. of IS&T/SID Eight Color Imaging Conference*, IS&T, Springfield, VA, pp.75-80, 2000.
33. [http://www.research.ibm.com/image\\_apps/capture.html](http://www.research.ibm.com/image_apps/capture.html)
34. H. S. Fairman, "Metameric correction using parametric decomposition", *Color Res. Appl.* **12**, pp. 261-265, 1997.